

Doubly-resonant-cavity electromagnetically induced transparency

Xin-Xin Hu^{1,2}, Chang-Ling Zhao^{1,2}, Zhu-Bo Wang^{1,2}, Yan-Lei Zhang^{1,2}, Xu-Bo Zou^{1,2},
Chun-Hua Dong^{1,2}, Hong X. Tang³, Guang-Can Guo^{1,2}, and Chang-Ling Zou^{1,2*}

¹ *Key Laboratory of Quantum Information, University of Science and
Technology of China, Hefei, 230026, People's Republic of China;*

² *Synergetic Innovation Center of Quantum Information & Quantum Physics,
University of Science and Technology of China, Hefei, Anhui 230026, China and*

³ *Department of Electrical Engineering, Yale University, New Haven, Connecticut 06511, USA*

(Dated: July 24, 2018)

We present an experimental study on the cavity-atom ensemble system, and realize the doubly-resonant cavity enhanced electromagnetically induced transparency, where both the probe and control lasers are resonant with a Fabry-Perot cavity. We demonstrate the precise frequency manipulating of the hybrid optical-atomic resonances, through either temperature or cavity length tuning. In such a system, the control power can be greatly enhanced due to the cavity, and all-optical switching is achieved with a much lower control laser power compared to previous studies. A new theoretical model is developed to describe the effective three-wave mixing process between spin-wave and optical modes. Interesting non-Hermitian physics are predicted theoretically and demonstrated experimentally. Such a doubly-resonant cavity-atom ensemble system without a specially designed cavity can be used for future applications, such as optical signal storage and microwave-to-optical frequency conversion.

I. INTRODUCTION

Near-resonance coherent light-atom interaction has been extensively studied [1, 2], because the atomic media promises the strong nonlinearity that cannot be achieved in dielectric materials. The strong nonlinearity is potential for the low intensity light-light interaction, which can be used for all-optical devices [3–6]. Usually, there are two approaches to enhance the coherent light-atom interaction, one is using the optical cavity to enable the light passing the atomic medium many times [7–10], and the other method is introducing atomic ensemble to collectively enhance the interaction strength [11–16].

In past two decades, great progresses have been achieved in such cavity-atomic ensemble system. Various nonlinear optics effects have been studied experimentally or theoretically, including the intracavity electromagnetically induced transparency (EIT) [17, 18], multiple laser thresholds [19], the photon blockade effect [20], strong and super-strong coupling [21], four-wave mixing [22], bistability [23, 24] and multi-stability [23, 25], as well as all-optical switching [23, 26–29]. However, in all previous experimental realizations of the all-optical switching, at most one cavity resonance for the signal light is used, while the control light is applied through free-space laser beam [17, 24, 27, 28]. Although the cavity resonance for the control light has the advantages that save the control laser power and are easy for control-signal alignment, there is an experimental challenge for realizing the cavity that doubly-resonant with two atomic transitions (e.g. 6.835 GHz for the D_2 line of ^{87}Rb). Because the frequency difference between two optical resonances is

determined by the cavity geometry, the doubly-resonant condition can only be satisfied with a specific cavity size.

In this work, we experimentally demonstrate the doubly-resonant Fabry-Perot (FP) cavity-atom ensemble system without specially designed cavity geometry, and achieve the all-optical switching with lower control power. We develop a new theoretical treatment, in which the resonances are actually the hybridized optical-atomic modes, to describe the effective three-wave mixing process for multiple-level atom couple with multiple cavity modes. Our theoretical analyses predict that the resonance frequency is tunable due to the dispersive effect of the atomic transitions and the nonlinearity of the Λ -type atom leads to non-Hermitian coupling between hybridized modes and spin-wave excitations. Benefiting from the different frequency shift rate for two hybridized modes by changing the cavity length, we experimentally demonstrated that the doubly-resonant condition can always be fulfilled by controlling of atom density and the effective detuning between the bare cavity resonances and atomic transitions. Based on this, we demonstrate the all-optical switching by the control laser, and study the extinction and response time of the switching. The demonstrated doubly-resonant cavity-atom ensemble system can boost the nonlinear interaction between light and spin excitation in the atom ensemble, can be used for other applications such as optical signal storage and readout [16, 30], and can also be generalized to other cavity systems and atom species.

II. THE SYSTEM AND PRINCIPLE

The scheme for the system is depicted in Fig. 1(a), in which a three-level atom ensemble is confined in an FP cavity and interacts with the cavity mode fields. If the

* clzou321@ustc.edu.cn

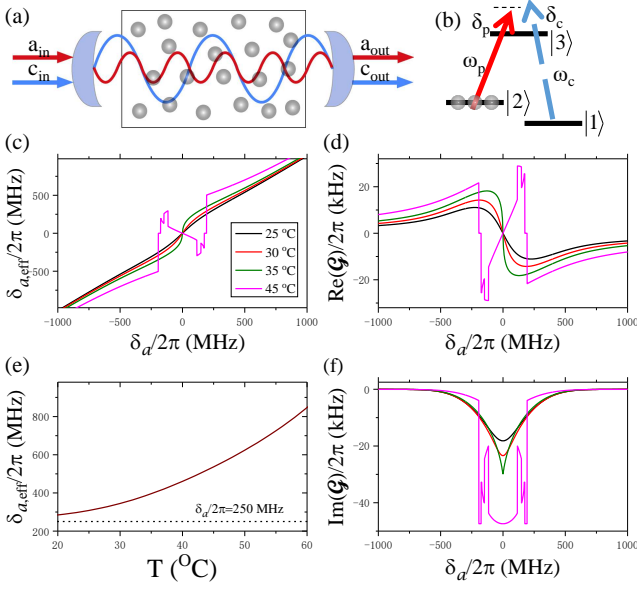


FIG. 1. (Color online) (a) Schematic illustration of the experimental system, consisting of an ensemble of ^{87}Rb that couples with two resonant modes in a Fabry-Perot cavity. (b) The energy diagram of the atomic system. Here, $|1\rangle$ and $|2\rangle$ are the two ground hyperfine states and $|3\rangle$ is the excited state of ^{87}Rb D_2 -transitions. ω_p and ω_c are the frequency of probe and control lasers with detunings δ_p and δ_c , respectively. (c) and (e) The dependence of δ_a^{eff} on the δ_a for given temperatures and on the temperature for a given $\delta_a/2\pi = 250$ MHz. (d) and (f) The real and imaginary parts of \mathcal{G} . The non-negligible imaginary part indicates the non-Hermitian interaction between the three modes.

transitions between ground hyperfine states and excited states (as shown in Fig. 1(b)) are near-resonant with cavity modes, the interaction between the external input optical field and the atoms can be greatly enhanced. The Hamiltonian for the cavity-atom ensemble can be written as ($\hbar = 1$)

$$\begin{aligned}
 H_0 &= \omega_a a^\dagger a + \omega_c c^\dagger c \\
 &+ \sum_j [(\omega_3 + kv_j) \sigma_{33,j} + \omega_2 \sigma_{22,j}] \\
 &+ \sum_j [g_{a,j} a \sigma_{32,j} + g_{c,j} c \sigma_{31,j} + h.c.] \quad (1)
 \end{aligned}$$

Here, $\sigma_{mn,j} = |m\rangle_j \langle n|$ with subscript j standing for j -th atom and $|1, 2, 3\rangle_j$ is the state of the atom as shown in Fig. 1(b). a and c are the Bosonic operators for probe and control cavity modes, respectively, with that the frequencies are ω_a and ω_c , respectively. $\omega_{3,j} = \omega_3 + kv_j$ is the frequency with Doppler shift for velocity of v_j , $k = \omega_3/v_c$ is the wave-vector and v_c is the velocity of light. $g_{a,j}$ ($g_{c,j}$) is the coupling strength between the atom transition and the cavity mode for the j -th atom.

From the Eq. (1), the three-level atoms mediate the nonlinear interaction between the two optical modes with

distinct frequencies. The cascading interactions $a\sigma_{32}$ and $c\sigma_{31}$ would leads to an effective process of $ac^\dagger\sigma_{12}$, i.e. the ground states of atoms have a flip when scattering the photons and change their color. To directly describe such process, we develop the effective three-wave mixing Hamiltonian in such a system. For our experiments, we have $g_{a,j}, g_{c,j} \ll \gamma_{23}, \gamma_{13}$, thus the excitation $\sigma_{33,j} \approx 0$ can be neglected, then we can solve the steady state of the system. Note that due to the coupling between the cavity mode and atom transitions, the cavity field is hybridized with the atomic excitation instead of the barely electromagnetic field of the photon. Then, we can solve the effective mode frequencies ω_a^{eff} and ω_c^{eff} for the hybridized cavity-atom ensemble modes, which satisfying

$$\begin{aligned}
 \sum_j \text{Im} \left[\frac{g_{a,j}^2 \sigma_{22,j}}{-i(\omega_{3,j} - \omega_2) - \gamma_{23} + i\omega_a^{\text{eff}}} \right] &= \omega_a - \omega_a^{\text{eff}}, \\
 \sum_j \text{Im} \left[\frac{g_{c,j}^2 \sigma_{11,j}}{-i\omega_{3,j} - \gamma_{13} + i\omega_c^{\text{eff}}} \right] &= \omega_c - \omega_c^{\text{eff}}.
 \end{aligned}$$

For hot atom ensemble, we have the sum over the ensemble corresponds to the integration over the three-dimensional space and three-dimensional momentum space, i. e. $\sum_j = \iiint \rho d^3\mathbf{x} \iiint P_{\text{MB}}(\mathbf{v}) d^3\mathbf{v}$. The Maxwell-Boltzman velocity distribution for v_z is $P_{\text{MB}}(v_z) = \sqrt{\frac{1}{2\pi\sigma_v}} \exp\left(-\frac{v_z^2}{2\sigma_v}\right)$, with $\int_{-\infty}^{\infty} P_{\text{MB}}(v_z) dv_z = 1$ and $\sigma_v = \frac{k_B T}{m}$. Introducing the function

$$\begin{aligned}
 F(\xi) &= \int dv_z \frac{P_{\text{MB}}(v_z)}{-ikv_z + \xi} \\
 &= \frac{1}{k} \sqrt{\frac{\pi}{2\sigma_v}} e^{\frac{\xi^2}{2k^2\sigma_v}} \left(1 - \text{erf}\left(\frac{\xi}{\sqrt{2\sigma_v}k}\right) \right), \quad (2)
 \end{aligned}$$

we have the characterization equations of the effective detunings as

$$\delta_a^{\text{eff}} - \delta_a + \sigma_{22} G_a \text{Im} [F(i\delta_a^{\text{eff}} - \gamma_{23})] = 0, \quad (3)$$

$$\delta_c^{\text{eff}} - \delta_c + \sigma_{11} G_c \text{Im} [F(i\delta_c^{\text{eff}} - \gamma_{13})] = 0, \quad (4)$$

where $\delta_a^{\text{eff}}(\delta_a) = \omega_a^{\text{eff}}(\omega_a) - \omega_3 + \omega_2$ and $\delta_c^{\text{eff}}(\delta_c) = \omega_c^{\text{eff}}(\omega_c) - \omega_3$ are the effective detuning between the hybrid cavity mode (original detuning between the bare cavity mode) and atomic transitions, and $G_{a,c} = \rho \iiint g_{a,c}^2(\mathbf{x}) d^3\mathbf{x}$. Introducing the collective spin wave operator

$$m = \sqrt{\rho} \frac{\iiint g_a(\mathbf{x}) g_c(\mathbf{x}) \sigma_{12}(\mathbf{x}) d^3\mathbf{x}}{\sqrt{\iiint g_a^2(\mathbf{x}) g_c^2(\mathbf{x}) d^3\mathbf{x}}}, \quad (5)$$

we obtain the effective Hamiltonian of the system

$$\begin{aligned}
 H_{\text{eff}} &= \omega_a^{\text{eff}} a^\dagger a + \omega_c^{\text{eff}} c^\dagger c + \omega_2 m^\dagger m \\
 &+ \mathcal{G} (a^\dagger c m^\dagger + a c^\dagger m), \quad (6)
 \end{aligned}$$

with the effective three-wave mixing coupling strength

$$\mathcal{G} = \sqrt{\rho \iiint g_a^2(\mathbf{x}) g_c^2(\mathbf{x}) d^3\mathbf{x}} \times F(i\delta_a^{\text{eff}} - \gamma_{23}). \quad (7)$$

The expression indicates that coupling strength \mathcal{G} would be a complex number, which corresponding to a non-Hermitian interaction between light and spin wave excitations [31]. Here, the $\text{Re}(\mathcal{G})$ is the coherent coupling strength originating from the coherent two-photon transition, while the $\text{Im}(\mathcal{G})$ is the incoherent coupling strength due to the spontaneous emission of excited state $|3\rangle$. In the following, the effects due to the interesting non-Hermitian mechanism would be revealed experimentally.

In our experimental configuration, there is a strong control field on mode c , thus approximately we have $\sigma_{11} \approx 0$, then $\omega_c^{\text{eff}} = \omega_c$. Including the control and probe laser fields, the system effective Hamiltonian in the rotating frame is

$$\begin{aligned} H = & (\delta_a^{\text{eff}} - \delta_p) a^\dagger a + (\delta_c - \delta_l) c^\dagger c \\ & + (\omega_2 + \delta_p - \delta_l) m^\dagger m + \mathcal{G} (a^\dagger c m^\dagger + a c^\dagger m) \\ & + (\sqrt{2\kappa_{a,1}} a_{in} a^\dagger + \sqrt{2\kappa_{c,1}} c_{in} c^\dagger + h.c.), \end{aligned} \quad (8)$$

with input laser detunings $\delta_p = \omega_p - \omega_3$ and $\delta_l = \omega_l - \omega_3 + \omega_2$, field amplitudes $a_{in} = \sqrt{P_p/\hbar\omega_p}$, $c_{in} = \sqrt{P_c/\hbar\omega_l}$, powers P_p and P_c , respectively. The external coupling rate to the cavity modes through the input mirror is $\kappa_{a(c),1}/2\pi = \frac{v_c}{4L} \frac{-\ln r}{2\pi}$, L is the length of the cavity and r is the reflectivity of the input mirror of the FP cavity (the reflectivity for modes a and c are almost the same). The steady state solution of the probe light transmittance ($\frac{d}{dt}a = \frac{d}{dt}c = 0$) is

$$t = \frac{2\sqrt{\kappa_{a,1}\kappa_{a,2}}}{-i(\delta_a^{\text{eff}} - \delta_p) - \kappa_a - \frac{n_c \mathcal{G}^2}{-i(\omega_2 + \delta_p - \delta_l) + \kappa_m}}. \quad (9)$$

Here, $n_c = 2\kappa_{c,1}c_{in}^2 / [(\omega_c - \omega_l)^2 + \kappa_c^2]$ is the intracavity control photon number, $\kappa_{a,2}$ is the coupling rate for the output mirror, with κ_a , κ_c and κ_m are the total loss rate of mode a , c and the collective spin wave excitation m , respectively.

From the equation, the transmission of the cavity mode can be modified by the control field. When $\delta_a^{\text{eff}} = \delta_l - \omega_2$ is satisfied, the modification of the probe field transmittance is most significant, which is proportional to three-wave interaction cooperativity $\mathcal{C} = n_c \mathcal{G}^2 / \kappa_a \kappa_m$. Therefore, there are additional two requirements for strong interaction: (1) the resonant condition $\delta_c - \delta_l = 0$ for control laser, since the n_c can be boosted by the on-resonant control field; (2) larger atom density ρ or higher temperature, since $\mathcal{G}^2 \propto \rho$.

The temperature dependent density of ^{87}Rb atoms can be estimated by $\rho(T) = 10^{7.738 - \frac{4215}{T}} / k_B T$ [32], thus we can numerically solve the δ_a^{eff} and \mathcal{G} with experimental parameters (explained in the next section). In Fig. 1(c), the δ_a^{eff} varies with the δ_a and shows nonlinear dependence when $\delta_a \sim 0$, as a result of the hybridization of the bare cavity and the atom ensemble. For higher temperature, the difference $\delta_a^{\text{eff}} - \delta_a$ becomes larger, and eventually shows strange shape due to the strong nonlinearity in dense atom ensemble. In Fig. 1(e), the dependence of

δ_a^{eff} on the temperature for given $\delta_a/2\pi = 250$ MHz is depicted. Both plots show that the δ_a^{eff} can be efficiently controlled by the bare cavity frequency and the atom vapor cell temperature, so there are two approaches to realize the doubly-resonant interaction. In addition, we also estimated the \mathcal{G} for different conditions [Fig. 1(d)&(f)], showing that the interaction is enhanced when the cavity is near-resonant with the atom and the temperature is increased. However, the \mathcal{G} shows non-negligible imaginary part, indicating the non-Hermitian interaction between the three modes, which would lead to new effect in such a system other than the traditional lossless three-wave coupling system [33–37].

III. EXPERIMENTAL SETUP

Our experimental setup is shown in Fig. 2. The standing-wave FP cavity with a length of 18 cm (FSR = 854 MHz) composes of two concave mirrors with the same curvature radius of 100 mm and reflectivity of 97% at 780 nm. One mirror is mounted on a piezoelectric transducer (PZT) to adjust the cavity length and can be locked into the control laser by a feedback loop. A glass vapor cell (Photonics Technologies, Rubidium-87) with a length of 75 mm, which is filled with pure ^{87}Rb gas and wrapped by a soft heater, is placed inside the cavity. The heater is controlled by a temperature controller (Thorlabs, TC200) to stabilize the temperature of the cell with the uncertainty less than 0.1 °C. Two external cavity diode lasers (Toptica DL100) are employed in the experiment, one for probe and the other one for control. The probe laser is coupled to the cavity through a standard polarization maintaining single-mode fiber (OZOptics), with the frequency continuously scanning cross the transitions between $5S_{1/2}$, $F = 2$ and $5P_{3/2}$, $F' = 1, 2, 3$ of ^{87}Rb . Similarly, the control laser is also coupled to the cavity, with the frequency locked around the transition from $5S_{1/2}$, $F = 1$ to $5S_{3/2}$, $F' = 1$ of ^{87}Rb by saturated absorption spectrum (SAS). The two lasers of orthogonal polarization are combined by a polarization beam splitter (PBS), and coupled to the cavity mirror. The beam profiles of both probe and control lasers are adjusted by an anti-reflection coated convex lens (focal length 25 mm) to match the fundamental transverse electromagnetic mode (TEM_{00}) of the optical cavity. The transmitted probe and control lasers through the cavity are separated by PBS and measured by two detectors (Thorlabs, PDA36A). In our experiment, we tested the FP cavity by measuring the transmission spectrum of the probe, and estimated the finesses of the cavity $\mathcal{F} = 21$ with cell placed in the cavity ($\mathcal{F} = 120$ without cell).

As discussed above, we should tune the cavity to find two modes with frequency differences being exactly the 6.835 GHz for the energy difference of ground hyperfine states. We have two strategies: (1) change the atom density of the cavity by changing the temperature of the vapor cell and (2) tune the cavity length.

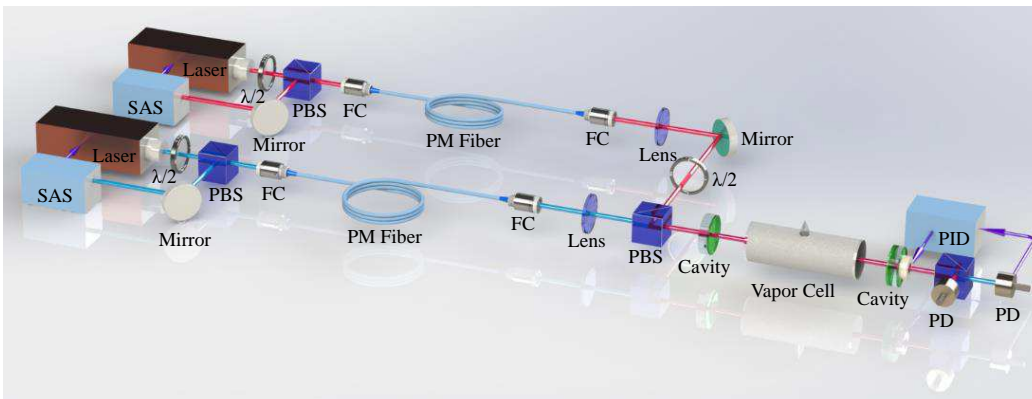


FIG. 2. (Color online) The experimental setup. Two external cavity diode lasers provide the probe and control lasers, which are locked by saturated absorption spectrum (SAS) and coupled into polarization-maintaining (PM) fibers. The FP cavity with the length of 18 cm composes of two concave mirrors with the same curvature radius of 100 mm and reflectivity of 97% at 780 nm. The cavity length is stabilized by the piezoelectric transducer and PID feedback loop. A glass vapor cell filled with pure ^{87}Rb is placed inside the cavity and covered with a soft heater (not shown here). Here, $\lambda/2$, PBS, FC, and PD means the half-wave plate, polarization beam splitter, fiber coupler, fiber and photon detector, respectively.

In the first approach, we lock the control laser to the frequency of the transition $5S_{1/2}, F = 1 \rightarrow 5P_{3/2}, F' = 1$, and then one of the cavity modes is locked to the control laser by the feedback based on the transmission of the control laser. When the temperature increases, the atom density in the cell increases, thus the cavity modes close to the probe $2 \rightarrow 3$ transition will strongly couple with the atoms, leading to the frequency shift, as predicted in Fig. 1(c) and (e). As shown in Fig. 3(a) and (b), by increasing the temperature, the frequency shifting increases. At specific temperature, we can find that the frequency difference between two modes be on-resonance with the $5S_{1/2}, F = 1 \rightarrow 5P_{3/2}, F' = 1$. Although the doubly-resonant cavity EIT has been observed [Fig. 2(b)], the optical modes for probe and control are both with high-loss and small transmittance. The reason is that the modes are too close to the atom transition frequencies leading to a strong absorption loss. From Fig. 2(a), the control mode almost disappears when the temperature approaches 40°C , and we can not lock the cavity by control mode above this temperature since the atom still induces considerable loss to the control mode with the residue population of the atom ensemble on $|2\rangle$.

The cavity spectrum for the other approach is shown in Fig. 3(c), where the control laser is locked with a frequency offset to the transition. In this case, both probe and control modes experience the strong coupling to the atom ensemble induced mode frequency shift for high atom density (temperature at 40°C). When changing the control mode frequency offset, the cavity length changes accordingly by the PZT. Benefiting from the hybridization with atom ensemble, the frequency shift rates for two modes by changing the cavity length are different, and we can always find a proper control frequency offset that the doubly-resonant condition can be fulfilled. Shown in Fig. 3(c) are the experimental results that the frequency spacing between two cavity modes can be tuned from

6.4 GHz to 7.0 GHz. The detailed EIT spectrum of the probe laser is shown in Fig. 3(d). Comparing to the first approach, due to the offset to the atom transitions, the absorption of atom ensemble will not be too strong and both the control and probe modes can maintain high-quality factor and large transmittance.

IV. DOUBLY-RESONANT CAVITY EIT

By the second approach, we locked the control mode to a specific frequency, which has a detuning of about 6.835 GHz with respect to the probe mode frequency, and realize the doubly-resonant condition at 40°C . To be more specific, the control laser is locked around the transition B in Fig. 3(c) and the probe laser is scanning around the probe mode close the transition A in Fig. 3(c). In the following experiments, the effective detuning for mode a is about 500 MHz at about 40 degrees, corresponds to the initial detuning of about 250 MHz. To verify the doubly-resonant cavity EIT, we measure the spectrum of the probe mode for various control laser powers, as shown in Fig. 4(a). As expected, there is a modification to the Lorentzian shape on the probe mode resonance when the probe laser frequency detuning to the control laser frequency matches the $\omega_2/2\pi \sim 6.835$ GHz. This can be explained that the reduced absorption by the control laser. According to our theory, the transmission of probe light can be estimated by Eq. (9). From the equation, the control laser induces an extra term $\frac{n_c G^2}{-i(\omega_2 + \delta_p - \delta_l) + \kappa_m}$, so effectively changing the intrinsic hybrid mode loss and frequency. For the on-resonance case $\delta_a^{\text{eff}} - \delta_p = 0$ and $\omega_2 + \delta_p - \delta_l = 0$, the maximum modification of the transmission (ratio between case with and

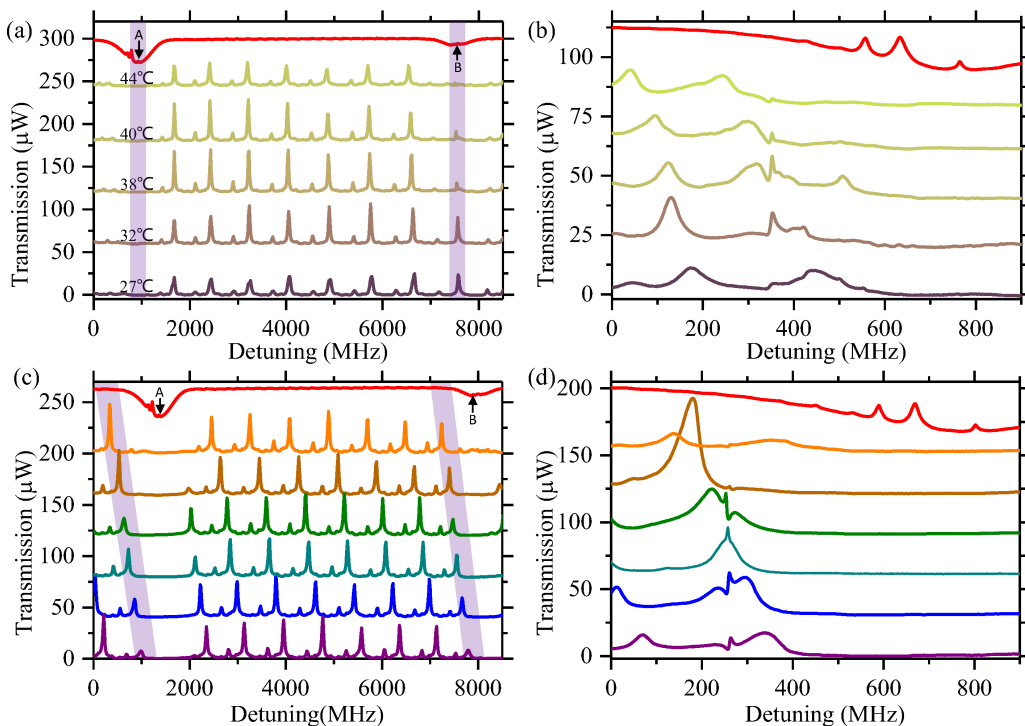


FIG. 3. (Color online) (a) The transmission of the cavity for different temperature with the control cavity mode and lasers are locked to the transition $5S_{1/2}, F = 1 \rightarrow 5P_{3/2}, F' = 1$. The red solid line is the saturated absorption spectrum for laser frequency calibration and others show the transmission of the cavity at the different temperature. The labels A and B denotes the two transitions $5S_{1/2}, F = 2 \rightarrow 5P_{3/2}, F' = 1$ and $5S_{1/2}, F = 1 \rightarrow 5P_{3/2}, F' = 1$, respectively. (b) is the detailed spectra of (a), showing the sharp modification of the spectrum due to the control field. (c) The transmission of cavity for different cavity length, with the temperature, stabilized at 40 °C. The effective signal mode detuning can be tuned by changing the cavity length, with the assistance of nonlinear dispersion by the cavity-atom ensemble hybridization. For appropriate cavity length, there are two modes with a frequency shift matching 6.835GHz and satisfying the doubly-resonant condition. The blue shade shows that the two modes have different frequency shifts at different cavity length. (d) is the detailed spectrum of (c) and an obvious EIT-lineshape can be observed. In this figure, spectra are plotted with equidistant bias for convenience.

without control) is

$$\eta = \left| \frac{1}{1+C} \right|^2 = \left| \frac{1}{1 + \frac{n_c \mathcal{G}^2}{\kappa_m \kappa_a}} \right|^2. \quad (10)$$

According to the traditional EIT without cavity [38], the control laser would reduce the absorption of the atomic medium, thus there is a control laser-induced transmission peak. However, for our system, the hybrid mode containing both atomic medium and photon with coherent feedback by the mirrors, the behaviors are essentially different from the cavity-less case. As indicated by Eq. (7), due to the spontaneous emission of the excited level $|e\rangle$, the effective coupling strength \mathcal{G} is a complex number, which leads to the non-Hermitian coupling between the collective spin wave mode and the hybrid optical modes. If \mathcal{G} is pure coherent coupling, i.e. is a real number, then $C > 0$ and the control laser will induce a dip in the transmission spectrum. If \mathcal{G} is pure incoherent coupling that hybrid mode frequency detuning is close to 0 (Fig. 1(f)), i.e. is an imaginary number, then $C < 0$ and there will be a peak in the transmission spectrum.

The results in Fig. 4(a) indicates that the incoherent coupling dominates, as there is always a peak induced by the control. To verify the model of our doubly-resonant system, we fitted the spectra. We found that the parameter $n_c \mathcal{G}^2 / P_c$ is a complex number, and shows relatively large fluctuation at low pump strength while approaches a steady state value when pump strength becomes larger. The fitted cavity linewidth is about 34 MHz, while the κ_m linearly increases with the control laser power, as shown in Fig. 4(c). This is consistent with our model that the control laser will induce an incoherent decay channel from the ground state $|1\rangle$ to $|2\rangle$. For the large fluctuation of parameters at low pump power, it can be attributed to the mechanism that the assumption of steady state population on level $|2\rangle$ is not valid for weak pump power.

V. ALL-OPTICAL SWITCHING

Based on the doubly-resonant cavity EIT, we can control the probe laser transmittance optically, which can be applied to realize the all-optical switching [23, 24, 26–

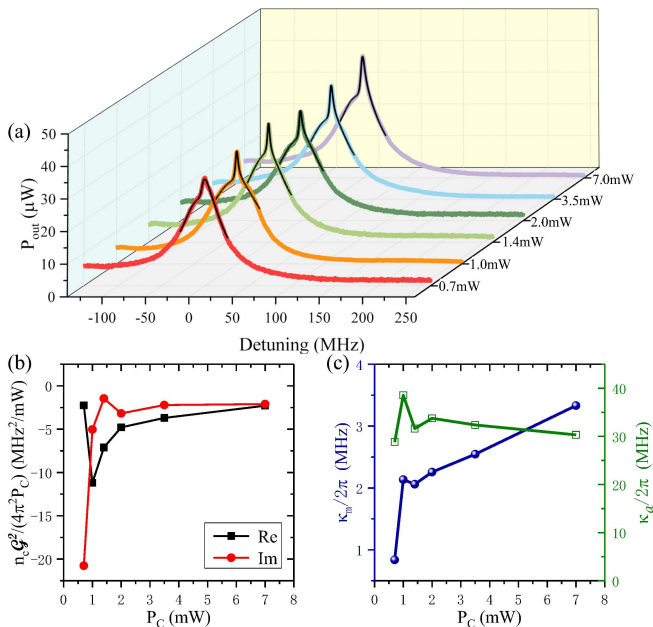


FIG. 4. (Color online) The transmission of the probe with different control laser power. (a) Enlarged spectrum under doubly-resonant condition. The spectra can be perfectly fitted by Eq. (7) (black solid line). (b) The real (black) and imaginary (red) part of the fitted parameter $n_c \mathcal{G}^2 / P_c$ against the control power, which effectively changes the intrinsic hybrid mode loss and frequency. (c) The fitted κ_m (blue line) and κ_a (green line) against the control power.

28]. Here, the probe laser is locked to the cavity resonance around the transition $5S_{1/2}, F = 2 \rightarrow 5P_{3/2}, F' = 1$, while the control lasers is locked to the transition $5S_{1/2}, F = 1 \rightarrow 5P_{3/2}, F' = 1$. The control laser is actually generated by a laser passing an AOM, and the control laser power and frequency are controlled by the RF driving on the AOM. So, the modulation of control laser is realized by modulating the RF power, with the RF frequency be adjusted to make the frequency difference between the control and the probe lasers matching the frequency difference between $5S_{1/2}, F = 1$ and $5S_{1/2}, F = 2$.

To characterize such a switch, we test the response of the transmitted probe laser for a square-wave control power modulation. During the experiments, the vapor cell is stabilized at a fixed temperature (40°C) and the input control power is fixed at 1.4 mW. The results as shown in Fig. 5(a) and (b) are the signal transmission with the control laser power modulation frequency of 1 kHz and 10 kHz, respectively. At low modulation rate, the signal transmission follows the control modulation, showing nice square-wave shape [Fig. 5(a)]. When the modulation rate is as large as 10 kHz, the signal transmission waveform deforms from the square-wave shape obviously [Fig. 5(b)]. Figure 5(c) depicts the contrast of signal transmittance against the switching rate. The all-optical switching extinction decreases when the modula-

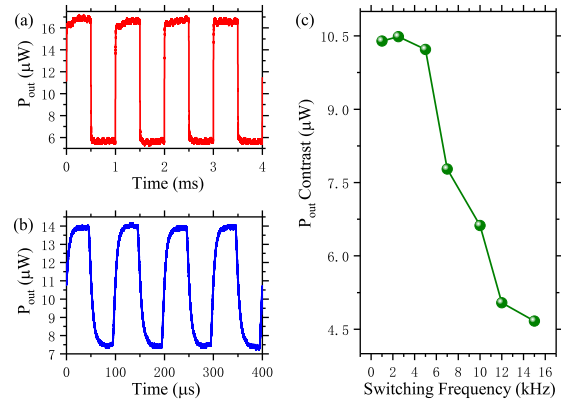


FIG. 5. (Color online) All-optical switching based on the doubly-resonant cavity EIT. (a) and (b) The temporal response of cavity signal transmission for square-wave control power modulation, with the modulation rate of 1 kHz and 10 kHz, respectively. (c) The contrast of the signal transmittance for different switching rate.

tion rate exceeds 8 kHz.

VI. DISCUSSION

Due to the impedance mismatching between the two cavity mirrors and the intracavity losses, most of the input probe and control laser power is reflected by the mirror. From the experimental results, the typical hybrid mode decay rate is $\kappa_a \sim 2\pi \times 34$ MHz, and the 97% reflectivity of the mirror leads to $\kappa_{a,1} = \kappa_{a,2} = 2\pi \times 2.0$ MHz, which means the reflection of input on-resonance probe or control laser is $R \approx \left| \frac{\kappa_a - 2\kappa_{a,1}}{\kappa_a} \right|^2 \sim 78\%$. This indicates it is possible to design an all-optical switching with weaker control power by choosing proper cavity mirror reflectivity to satisfy the impedance matching condition. The on-off ratio of the switch η could be improved for higher \mathcal{C} , but it is limited by the saturated cooperativity $\mathcal{C} = \frac{n_c \mathcal{G}^2}{\kappa_m \kappa_a}$ because κ_m also increases with n_c . As a result, the EIT peak height saturated for large pump power in Fig. 4(a) (the estimation of saturated $\eta \sim 1.37$ for our experimental results). In addition, the rate of the switching is limited by the atom flying effect. After turning on the laser, the population of the atom ensemble reaches the steady state after all the atoms passing through the control laser. The vapor cell we used currently has an average flying time of about 42 μs , corresponding to a relaxation rate of the order of 3.8 kHz, which agrees with the curve shown in Fig. 5(c).

The possible approaches to improve the performance of the switching include optimizing the cavity to reduce the intrinsic loss of the hybrid mode due to the scattering and absorption of vapor cell wall, and optimizing the δ_a to minimize the control light inducing collective spin wave

relaxation. Besides, we do not shield the magnetic field induced by earth or spin relaxation due to the collision to the cell wall. If we add magnetic shields around ^{87}Rb vapor cell and also anti-relaxation coating in the cell, the linewidth of the EIT will decrease significantly and the extinction will be greatly enhanced.

The doubly-resonant condition can actually enable the cavity-enhanced photon-spin wave coupling, thus we expect this method be used for quantum memory with reduced control power. This doubly-resonant cavity EIT switch may also be generalized to a more compact platform, such as integrated photonic circuits [39–41]. For smaller cavity, the FSR is much larger than the ground state splitting, but we can explore the modes of different polarization to satisfy the doubly-resonant condition. In addition, adding an external bias magnetic field will lift the degeneracy of the transitions and adjust the split between two modes. Therefore the doubly-resonant cavity-atom ensemble coupling can be achieved in the microcavity easily.

VII. CONCLUSION

In summary, we theoretically and experimentally studied the electromagnetically induced transparency of a

cavity-atom ensemble system, in which the transitions of two ground states of ^{87}Rb D_2 line are on-resonant with two fundamental modes of the cavity. We demonstrate two approaches that can precisely tune the hybrid cavity mode frequencies to achieve the doubly-resonant condition. We measure and analyze the effect of all-optical switching based on the doubly-resonant cavity EIT, and realized a switching extinction of about 46% at a rate of 10 kHz. The developed theoretical treatment of the three-wave mixing between spin-wave and optical modes would find application in future microwave-to-optical frequency conversion, and the revealed incoherent coupling may stimulate further studies on non-Hermitian physics by exploring such as cavity-atom ensemble system.

ACKNOWLEDGMENTS

We thank Pengfei Zhang, Xudong Yu, Tian Xia, Yanhong Xiao, Chuan-Sheng Yang for fruitful discussions. This work was supported by the National Key R & D Program (Grant No.2016YFA0301300, 2017YFA0304504 and 2016YFA0301700), National Natural Science Foundation of China (Grant No. 61505195 and 91536219), and Anhui Initiative in Quantum Information Technologies (AHY130000).

-
- [1] M. Lukin, “Colloquium: Trapping and manipulating photon states in atomic ensembles,” *Rev. Mod. Phys.* **75**, 457 (2003).
- [2] K. Hammerer, A. S. Sørensen, and E. S. Polzik, “Quantum interface between light and atomic ensembles,” *Rev. Mod. Phys.* **82**, 1041 (2010).
- [3] M. Bajcsy, S. Hofferberth, V. Balic, T. Peyronel, M. Hafezi, A. S. Zibrov, V. Vuletić, and M. D. Lukin, “Efficient All-Optical Switching Using Slow Light within a Hollow Fiber,” *Phys. Rev. Lett.* **102**, 203902 (2009).
- [4] B. Wu, J. F. Hulbert, E. J. Lunt, K. Hurd, A. R. Hawkins, and H. Schmidt, “Slow light on a chip via atomic quantum state control,” *Nat. Photonics* **4**, 776 (2010).
- [5] T. Peyronel, O. Firstenberg, Q.-Y. Liang, S. Hofferberth, A. V. Gorshkov, T. Pohl, M. D. Lukin, and V. Vuletić, “Quantum nonlinear optics with single photons enabled by strongly interacting atoms,” *Nature* **488**, 57 (2012).
- [6] V. Venkataraman, K. Saha, and A. L. Gaeta, “Phase modulation at the few-photon level for weak-nonlinear-based quantum computing,” *Nat. Photonics* **7**, 138 (2013).
- [7] R. J. Thompson, G. Rempe, and H. J. Kimble, “Observation of normal-mode splitting for an atom in an optical cavity,” *Phys. Rev. Lett.* **68**, 1132 (1992).
- [8] K. M. Birnbaum, A. Boca, R. Miller, A. D. Boozer, T. E. Northup, and H. J. Kimble, “Photon blockade in an optical cavity with one trapped atom,” *Nature* **436**, 87 (2005).
- [9] P. Zhang, Y. Guo, Z. Li, Y. Zhang, Y. Zhang, J. Du, G. Li, J. Wang, and T. Zhang, “Elimination of the degenerate trajectory of a single atom strongly coupled to a tilted TEM₁₀ cavity mode,” *Phys. Rev. A* **83**, 031804 (2011).
- [10] B. Hacker, S. Welte, G. Rempe, and S. Ritter, “A photon-photon quantum gate based on a single atom in an optical resonator,” *Nature* **536**, 193 (2016).
- [11] M. G. Raizen, R. J. Thompson, R. J. Brecha, H. J. Kimble, and H. J. Carmichael, “Normal-mode splitting and linewidth averaging for two-state atoms in an optical cavity,” *Phys. Rev. Lett.* **63**, 240 (1989).
- [12] Y. Zhu, D. J. Gauthier, S. E. Morin, Q. Wu, H. J. Carmichael, and T. W. Mossberg, “Vacuum Rabi splitting as a feature of linear-dispersion theory: Analysis and experimental observations,” *Phys. Rev. Lett.* **64**, 2499 (1990).
- [13] Min Xiao, “Novel linear and nonlinear optical properties of electromagnetically induced transparency systems,” *IEEE J. Sel. Top. Quantum Electron.* **9**, 86 (2003).
- [14] H. Tanji-Suzuki, I. D. Leroux, M. H. Schleier-Smith, M. Cetina, A. T. Grier, J. Simon, and V. Vuletić, *Adv. At. Mol. Opt. Phys.*, Vol. 60 (2011) pp. 201–237.
- [15] J. Jing, Z. Zhou, C. Liu, Z. Qin, Y. Fang, J. Zhou, and W. Zhang, “Ultralow-light-level all-optical transistor in rubidium vapor,” *Appl. Phys. Lett.* **104**, 151103 (2014).
- [16] J. Simon, H. Tanji, J. K. Thompson, and V. Vuletić, “Interfacing Collective Atomic Excitations and Single Photons,” *Phys. Rev. Lett.* **98**, 183601 (2007).
- [17] H. Wu, J. Gea-Banacloche, and M. Xiao, “Observation of Intracavity Electromagnetically Induced Transparency and Polariton Resonances in a Doppler-Broadened Medium,” *Phys. Rev. Lett.* **100**, 173602 (2008).

- [18] G. Hernandez, J. Zhang, and Y. Zhu, “Collective coupling of atoms with cavity mode and free-space field,” *Opt. Express* **17**, 4798 (2009).
- [19] C. Fang-Yen, C. C. Yu, S. Ha, W. Choi, K. An, R. R. Dasari, and M. S. Feld, “Observation of multiple thresholds in the many-atom cavity QED microlaser,” *Phys. Rev. A* **73**, 041802 (2006).
- [20] C. Guerlin, E. Brion, T. Esslinger, and K. Mølmer, “Cavity quantum electrodynamics with a Rydberg-blocked atomic ensemble,” *Phys. Rev. A* **82**, 053832 (2010).
- [21] X. Yu, D. Xiong, H. Chen, P. Wang, M. Xiao, and J. Zhang, “Multi-normal-mode splitting of a cavity in the presence of atoms: A step towards the superstrong-coupling regime,” *Phys. Rev. A* **79**, 061803 (2009).
- [22] X. Yu, M. Xiao, and J. Zhang, “Triply-resonant optical parametric oscillator by four-wave mixing with rubidium vapor inside an optical cavity,” *Appl. Phys. Lett.* **96**, 041101 (2010).
- [23] H. Wang, D. Goorskey, and M. Xiao, “Controlling light by light with three-level atoms inside an optical cavity,” *Opt. Lett.* **27**, 1354 (2002).
- [24] R. Sawant and S. A. Rangwala, “Optical-bistability-enabled control of resonant light transmission for an atom-cavity system,” *Phys. Rev. A* **93**, 023806 (2016).
- [25] A. Joshi and M. Xiao, “Optical Multistability in Three-Level Atoms inside an Optical Ring Cavity,” *Phys. Rev. Lett.* **91**, 143904 (2003).
- [26] A. M. C. Dawes, “All-Optical Switching in Rubidium Vapor,” *Science* **308**, 672 (2005).
- [27] X. Wei, J. Zhang, and Y. Zhu, “All-optical switching in a coupled cavity-atom system,” *Phys. Rev. A* **82**, 033808 (2010).
- [28] S. Dutta and S. A. Rangwala, “All-optical switching in a continuously operated and strongly coupled atom-cavity system,” *Appl. Phys. Lett.* **110**, 121107 (2017).
- [29] L. Wang, K. Di, Y. Zhu, and G. S. Agarwal, “Interference control of perfect photon absorption in cavity quantum electrodynamics,” *Phys. Rev. A* **95**, 013841 (2017).
- [30] M. Hosseini, B. M. Sparkes, G. Campbell, P. K. Lam, and B. C. Buchler, “High efficiency coherent optical memory with warm rubidium vapour,” *Nat. Commun.* **2**, 174 (2011).
- [31] R. El-Ganainy, K. G. Makris, M. Khajavikhan, Z. H. Musslimani, S. Rotter, and D. N. Christodoulides, “Non-Hermitian physics and PT symmetry,” *Nat. Phys.* **14**, 11 (2018).
- [32] P. Siddons, C. S. Adams, C. Ge, and I. G. Hughes, “Absolute absorption on rubidium D lines: comparison between theory and experiment,” *J. Phys. B At. Mol. Opt. Phys.* **41**, 155004 (2008).
- [33] S. Weis, R. Riviere, S. Deleglise, E. Gavartin, O. Arcizet, A. Schliesser, and T. J. Kippenberg, “Optomechanically Induced Transparency,” *Science* **330**, 1520 (2010).
- [34] V. Singh, S. J. Bosman, B. H. Schneider, Y. M. Blanter, A. Castellanos-Gomez, and G. a. Steele, “Optomechanical coupling between a multilayer graphene mechanical resonator and a superconducting microwave cavity,” *Nat. Nanotechnol.* **9**, 820 (2014).
- [35] X. Zhang, C.-l. Zou, L. Jiang, and H. X. Tang, “Strongly coupled magnons and cavity microwave photons,” *Phys. Rev. Lett.* **113**, 156401 (2014).
- [36] L. Fan, K. Y. Fong, M. Poot, and H. X. Tang, “Cascaded optical transparency in multimode-cavity optomechanical systems,” *Nat. Commun.* **6**, 5850 (2015).
- [37] K. C. Balram, M. I. Davanço, J. D. Song, and K. Srinivasan, “Coherent coupling between radiofrequency, optical and acoustic waves in piezo-optomechanical circuits,” *Nat. Photonics* **10**, 346 (2016).
- [38] A. J. Olson and S. K. Mayer, “Electromagnetically induced transparency in rubidium,” *Am. J. Phys.* **77**, 116 (2009).
- [39] R. Ritter, N. Gruhler, W. H. P. Pernice, H. Kübler, T. Pfau, and R. Löw, “Coupling thermal atomic vapor to an integrated ring resonator,” *New J. Phys.* **18**, 103031 (2016).
- [40] L. Stern, R. Zektzer, N. Mazurski, and U. Levy, “Enhanced light-vapor interactions and all optical switching in a chip scale micro-ring resonator coupled with atomic vapor,” *Laser Photon. Rev.* **10**, 1016 (2016).
- [41] L. Stern, B. Desiatov, N. Mazurski, and U. Levy, “Strong coupling and high-contrast all-optical modulation in atomic cladding waveguides,” *Nat. Commun.* **8**, 14461 (2017).